

Synthesis, Structural, Optical, Thermal and Electrical Properties of Urea Sulphamic Acid (USA) Single Crystal

E. Chinnasamy, N. Indumathi, S. Senthil*

Department of Physics, Government Arts College for Men, Nandanam, Chennai, Tamil Nadu, India

ABSTRACT

Single crystals of Urea Sulphamic acid (USA) have been grown by the slow evaporation technique at room temperature using aqueous solution. The single crystal PXRD study confirms orthorhombic p system for the grown crystal. The functional groups present in the grown crystal have been identified by FTIR and FT-Raman analyses. The optical properties of the USA crystal were determined using UV-Visible spectroscopy. Optical constants such as the reflectance, the refractive index, the extinction coefficient, electric susceptibility were determined from UV-Visible spectroscopy. The thermal stability of the crystal was determined from thermo gravimetric and differential thermal analysis curve. The dielectric constant and the dielectric loss were measured as a function of different frequencies and temperatures. The AC electrical conductivity study revealed that the conduction depended both on the frequency and the temperature.

Keywords: Urea sulphamic acid, Single X-ray diffraction, FT-IR, Optical transmission, Dielectric studies.

I. INTRODUCTION

Organic based materials have great promise in electronics due to the ease of their design and synthesis to suit the requirements of optoelectronic technologists. In order to be useful in modern technology, the material should possess large second order optical nonlinearity, short transparency cut-off wavelength and good thermal stability. In this era of photonics and lasers, organic molecules are capable of influencing photonic signal efficiency in technologies such as optical communication, optical computing and dynamic image processing. The versatility of organic materials is due to their superior properties such as higher susceptibility, faster response and flexibility [1-2]. Organic NLO materials are of current interest due to their more favorable nonlinear response and molecular structure flexibility. The unique optoelectronic properties of organics are due to the formation of weak Vanderwaals and hydrogen bonds and hence show high degree of localization. Urea is one of such organic NLO materials which have been

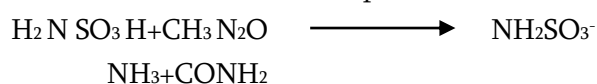
explored as a first for NLO device for second and fifth harmonic generation [3]. In addition to this, the potentiality of urea as a first organic parametric oscillator [4], having extended transparency in the UV region, large birefringence, high optical damage threshold [5-6] etc. makes it an attractive material. Sulphamic acid (SA) is a classical inorganic compound which exhibits orthorhombic structure with the space group P_{bca} . The crystal growth and detailed studies on (SA) crystal reveal the ability of (SA) for optoelectronic device fabrications [7].

In the present work, Urea Sulphamic acid (USA), a desirable organic nonlinear optical crystal, has been grown from aqueous solution using slow evaporation technique. The grown crystals were subjected to various characterizations such as single crystal X-ray diffraction analysis, Fourier Transform Infrared FTIR and Raman analysis, optical absorption studies, TG/DTA, dielectric constant and the dielectric loss were measured as a function of different frequencies and temperatures. The AC electrical conductivity

study revealed that the conduction depended both on the frequency and the temperature.

II. EXPERIMENTAL PROCEDURE

Urea Sulphamic acid was synthesized by taking commercially available (AR grade E-Merck) urea and sulphamic acid in the stoichiometric ratio of 2:1 and dissolved in deionised Water at room temperature. The resulting solution was stirred well for about 3 hours using a magnetic stirrer to attain a homogeneous mixture. The expected reaction mechanism for this title compound is



Suspended impurities from the solution were removed using high quality Whatmann filter paper. The filtered solution was then transferred into 100 ml beaker. To control the evaporation of the solution, it was covered with a perforated polythene sheet. After 25 days, good quality crystals were harvested with dimensions of 35 x 24 x 15 mm³. Figure 1(a). Shows optically clear (USA) crystal grown by the slow evaporation method.



Figure 1(a). Photograph of as grown crystal of USA

III. RESULTS AND DISCUSSION

3.1 Single and powder X-ray diffraction study
Single crystal X-ray diffraction analysis of (USA) crystal were carried using an Enraf Nonius CAD4 single crystal X-ray diffractometer with an incident CuK α radiation ($\lambda=0.7107 \text{ \AA}$) for the grown crystal. It is confirmed from this study that the title compound crystallizes in orthorhombic p system. From the XRD

data the calculated lattice parameter values are found to be $a= 8.076 \text{ \AA}$, $b= 8.098 \text{ \AA}$, $c= 9.218 \text{ \AA}$, $\alpha=\beta=\gamma=90^\circ$ and $V = 602.8 (\text{A}^3)$. Powder X-ray diffraction analysis has been carried out using Philips Powder X-ray diffractometer using CuK α radiation to identify the lattice parameters. The sharp and well defined Bragg's peaks confirmed the crystallinity of the grown crystals. Powder X-ray diffraction pattern of the grown crystal was shown in Figure 2.

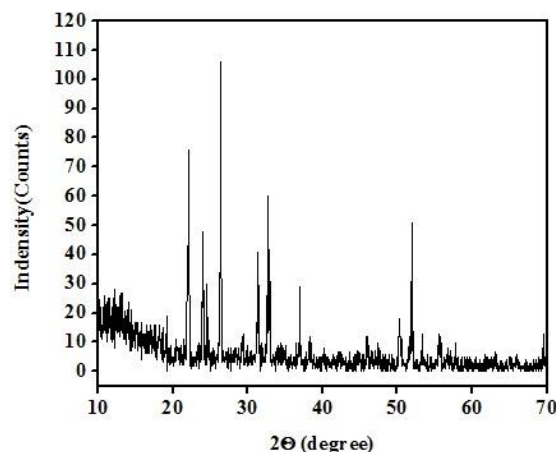


Figure 2. Powder XRD pattern of USA

3.2. FTIR and Raman spectral analysis

FTIR spectral studies have been carried out to characterize the functional groups of the grown (USA) crystal shown in (Figure. 3(a)). The band at 3096, 2877, cm^{-1} corresponds to NH_3^+ stretching vibration. The presence of bands between 2561, 2455 cm^{-1} are mainly due to N-H stretching. The band observed at 1740 cm^{-1} arises from symmetric vibration of NH_3^+ group and the band at 1440 cm^{-1} is assigned to the asymmetric stretching of NH_3^+ mode. The stretching of SO_3^- may be assigned to the vibration at 1239 cm^{-1} . The strong band at 1061 cm^{-1} corresponds to the C-N stretching vibration. The bands at 1001, 683, 555 cm^{-1} are due to NH_3^+ rocking, N-S stretching and SO_3^- deformation respectively. The presence of functional group was further confirmed by Raman spectrum shown in (Figure. 3(b)). the peak at 1519 cm^{-1} is due to NH_3^+ deformation. The peaks at 1339, 1302 cm^{-1} are due to the presence of SO_3^- stretching and N-H...S bond respectively. Strong peak at 1056 cm^{-1} is due to C-O stretching, this peak was also observed at FTIR

spectrum. It shows that these vibrations are both IR and Raman active. The NH₂ and N-H stretching vibration appeared around 699,678 cm⁻¹. The peaks observed at 555, 520 cm⁻¹ are due to SO₃⁻ rocking and N-S torsion respectively.

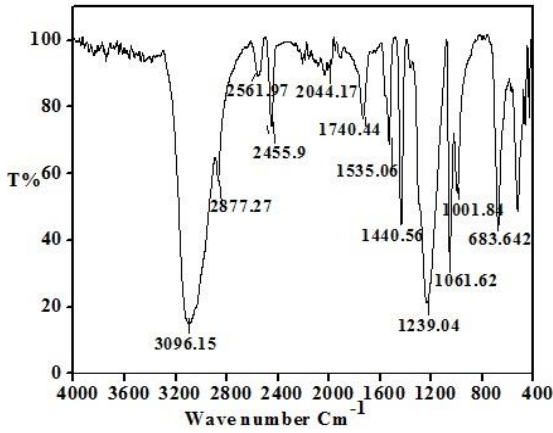


Figure 3(a). FTIR spectrum of USA.

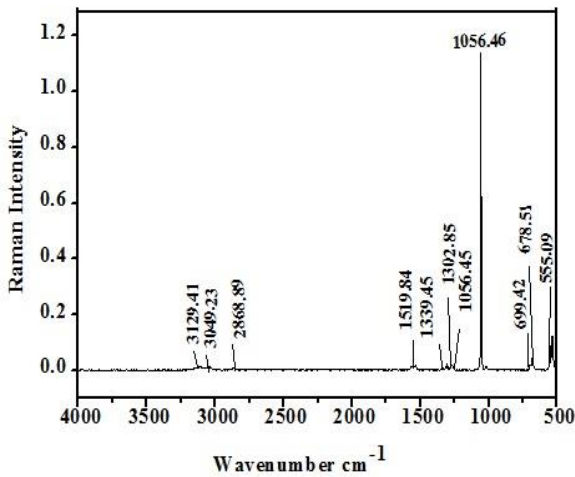


Figure 3(b). Raman spectrum of USA

3.3. UV-Vis absorption study

The absorbance band, transparency cut-off and transmission range are the important optical parameters for laser frequency conversion applications [8]. The linear optical property of the grown (USA) crystal was studied using LAMBDA-35 UV-Visible spectrophotometer. The spectrum obtained is depicted in Figure. 4(a). UV-Visible spectral analysis gives useful information about electronic transitions of the compound and is assisted to understand the electronic structure and optical band gap of the crystal [9]. From

the spectrum, it is noticed that the absorption of the crystal is considerably low in the wavelength region and prominent peaks observed in the spectrum may be due to overtones or the combination bands of either stretching or bending vibration in the UV region. The optical cut-off wavelength of the crystal was found to be 269 nm. The low absorption in the entire visible region clearly confirms its suitability for the fabrication of nonlinear optical devices.

3.3.1. Optical band gap

The optical constants of the material such as forbidden energy band gap and refractive index are necessary for optical and optoelectronic applications. The optical absorption coefficient (α) was calculated from the measured transmittance (T) using the relation

$$\alpha = \frac{2.303 \log\left(\frac{1}{T}\right)}{t} \quad (1)$$

Where T is the transmittance and t is the thickness of the crystal.

The optical absorption coefficient (α) near the absorption edge is predicted by the following relation

$$h\nu\alpha = A(h\nu - E_g)^{1/2} \quad (2)$$

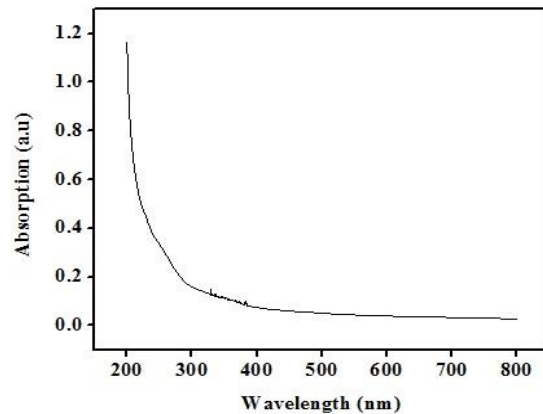


Figure 4(a). UV-Vis spectrum

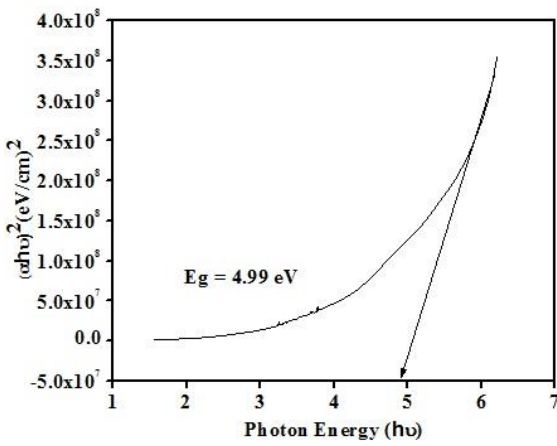


Figure 4(b). Tauc's plot of $(\alpha hv)^2$ against photon energy (hv)

where E_g is the optical band gap of the crystal, A is a constant, h is the Planck's constant and ν is the frequency of the incident photon. The Tauc's plot of $(\alpha hv)^2$ against photon energy (hv) is shown in Figure. 4(b). The optical band gap was estimated by the extrapolation of the linear part of the plot and the band gap energy was calculated as 4.99 eV. Being a wide band gap and large transmittance in the UV-Vis region, it clearly confirms the dielectric nature of the material [10].

3.3.2. Optical constant determination

The prominent way to gain the potential of the material is getting knowledge of optical constants of the material. The finding of optical parameters was determined using the following theoretical formulas [11]. The extinction coefficient (K) is given by

$$K = \frac{\alpha \lambda}{4\pi} \quad (3)$$

The reflectance (R) in terms of absorption coefficient (α) and the refractive index (n) in terms of reflectance (R) can be derived from the relation [12],

$$R = 1 \pm \frac{\sqrt{1 - \exp(-\alpha t) + \exp(\alpha t)}}{1 + \exp(-\alpha t)} \quad (4)$$

$$N = - \left\{ \frac{(R+1) \pm \sqrt{3R^2 + 10R - 3}}{2(R-1)} \right\} \quad (5)$$

With the aid of absorption spectra, the linear optical constants such as extinction coefficient, reflectance and refractive index of (USA) single crystal were calculated from the above expressions and the variation of reflectance, extinction coefficient and refractive index as a function of photon energy is plotted as shown in Figures. 5(a)–5(c), respectively. It is observed that the extinction coefficient and reflectance purely depend on the photon energy. The refractive index is an important parameter for the measure of intensity of reflected light and the plot along refractive index and photon energy is depicted in Figure. 5(c) and the refractive index is calculated to be 1.76. Figure 5(d) represents the twain reflectance and extinction coefficient dependence on absorption coefficient. The internal energy of the material is completely dominated on this absorption coefficient.

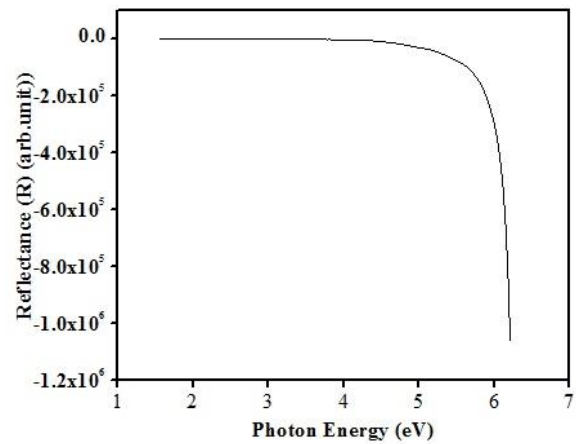


Figure 5(a). Photon energy versus reflectance R

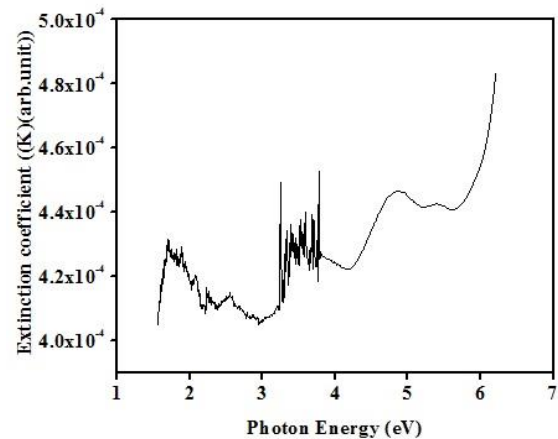


Figure 5(b). Extinction coefficient K

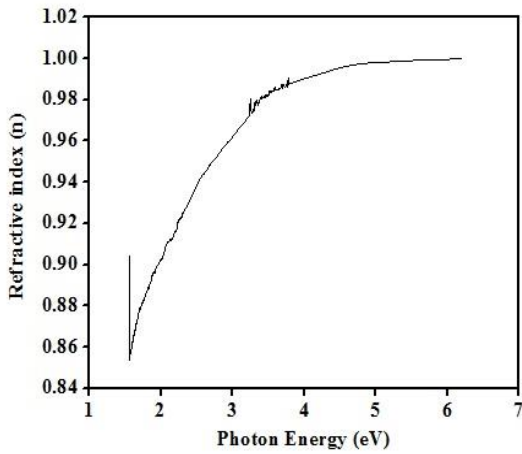


Figure 5(c). Refractive index n

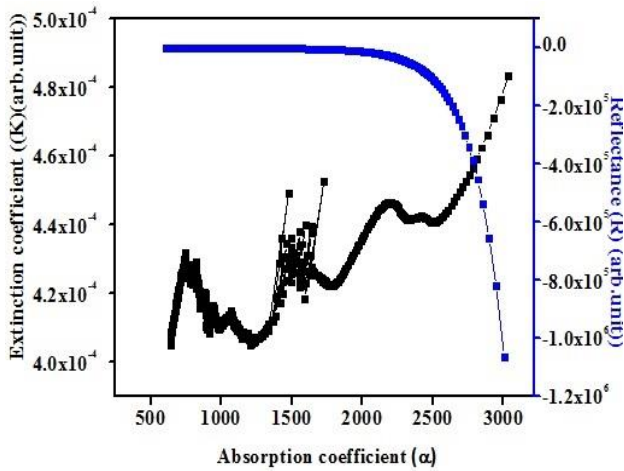


Figure 5(d). Absorption coefficient (α) versus reflectance R and extinction coefficient K

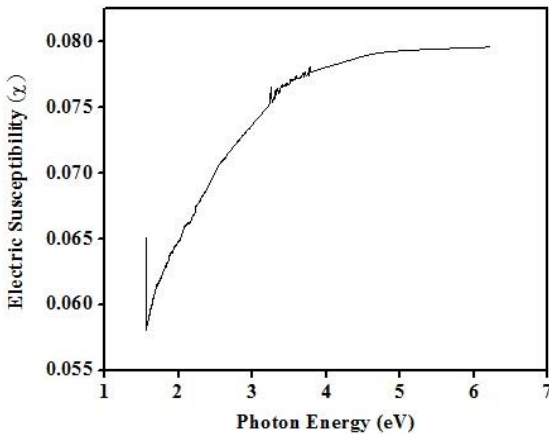


Figure 6(a). Plot of photon energy versus susceptibility.

The electrical susceptibility was assessed from the refractive index of the crystal according to the formula

$$\epsilon_r = \epsilon_0 + 4\pi\chi_c = n^2 - K^2, \tag{6}$$

$$\chi_c = \frac{n^2 - k^2 - \epsilon_0}{4\pi} \tag{7}$$

where ϵ_0 is the dielectric constant in the absence of any contribution from free carriers. Also, the complex dielectric constant could be worked out from

$$\epsilon_r = n^2 - k^2, \quad \epsilon_i = 2nk. \tag{8}$$

The plot of photon energy versus susceptibility for (USA) single crystal is shown in Figure. 6(a). Thus, the optical constants of the material with high band gap energy and low extinction coefficient and refractive index elucidate the suitability for device applications in processing and computing optical data [13].

3.4 Thermal Analysis

The thermal behavior of USA was examined by thermogravimetric analysis (TG) and differential thermal analysis (DTA) using the USA sample of 7 mg at the beginning. A thermal analyzer was employed at a heating rate 20°C/min in the nitrogen atmosphere. The thermogram obtained from TG and DTA analyses recorded at 20-500°C are shown in Figure. 7. The TGA spectrum indicates that there is no weight loss up to 150°C which confirms the absence of water of crystallization in the title compound. There after weight loss occurs in a single step between 150°C to 475°C which gradually decreases to zero weight. Differential thermal analysis (DTA) curve shows two endothermic peaks. It implies that the material undergoes an exothermic transition at 191.0 °C, which promptly indicate the first stage of decomposition of the material, coincides well with the TGA spectrum. The second endothermic peak at 409.4°C may be due to the decomposition and volatilization of the compound. After that no sharp peak was observed, which confirms that the material is thermally stable up to 409.4°C.

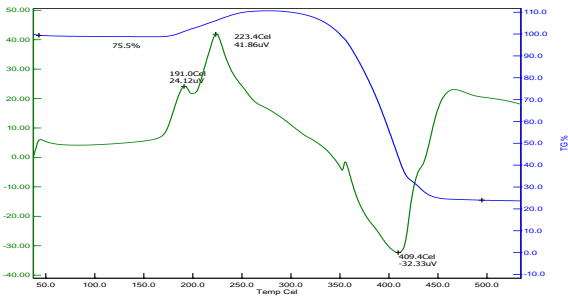


Figure 7. TG/DTA curve for USA single crystal.

3.5 Dielectric materials

Dielectric properties give information about the electric field distribution, the nature of atoms, polarization mechanisms and quality of the material. The dielectric constant of the material also depicts the movement of charges during polarization process. The dielectric characteristics of (USA) were executed for various temperatures from 50Hz to 5MHz frequency range. The dielectric permittivity and dielectric loss of the material has been studied from the following relation:

$$\epsilon' = \frac{C_d}{A\epsilon_0} \quad (9)$$

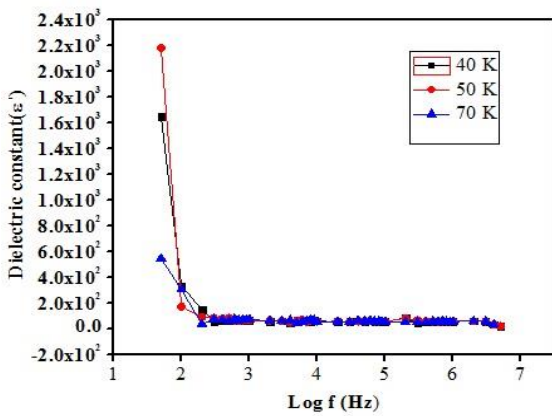


Figure 8(a). Plot of log f versus dielectric constant

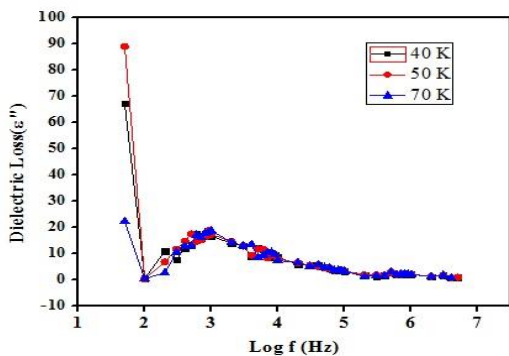


Figure 8(b). Plot of log f versus dielectric loss.

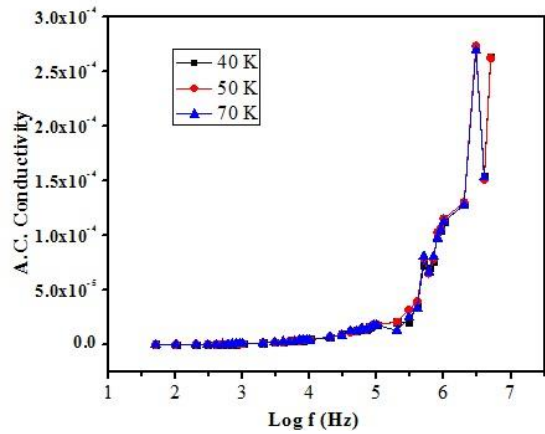


Figure 8(c). Plot of log ω versus log σ_{ac}.

where C represents the capacitance, d the thickness of the sample, A the area of sample and ε₀ the dielectric constant in vacuum. The variations of dielectric constant and dielectric loss in terms of frequency at few selected temperatures are shown in Figure 8. The graph clearly narrates that in the low frequency region the dielectric constant has a high value and decreases exponentially towards the high frequency region and attains constant for all temperatures. The high value of dielectric constant at low frequencies might be due to all polarizations especially the ionic and space charge polarizations [14]. At high frequency, the space charge polarization cannot withstand due to the lack of ability of dipoles causing a decrease in dielectric constant of the material. Eventually, the low value of dielectric constant and dielectric loss of the material enhances good optical quality with much lesser defects.

3.5.1. AC conductivity

The AC conductivity σ_{ac} is formulated using the relation:

$$\sigma_{ac} = 2\pi f \epsilon_0 \epsilon' \tan\delta \quad (10)$$

Where f denotes the frequency of the applied ac field (Hz). The conduction mechanism is understood from the graph of log σ_{ac} versus log ω at various temperatures and represented in Figure. 8(c). Hence the low frequency conductivity data define a little variation which predicts the frequency independent

part; σ_{dc} could be associated with irregular diffusion of the ionic charge carriers via activated hopping [15]. The conductivity spectrum exhibits dispersion at higher frequencies, thus showing the onset of ac conductivity. Also at higher frequencies, the ionic conductivity increases with the increasing frequency which may be ascertained to the forward and backward ion displacements occurring simultaneously.

IV. CONCLUSION

Urea Sulphamic acid (USA) crystals have been successfully grown from aqueous solution by the slow evaporation solution growth technique. The cell parameters of USA crystal were determined from Single and powder X-ray diffraction studies. FTIR and Raman spectra identified the functional groups in material. The optical cut-off wavelength of the crystal have been found to be 269 nm, band gap (4.99 eV), extinction coefficient, etc of transparent USA crystals were determined in UV-vis studies which suggested the suitability of material for optoelectronics applications. The TG/ DTA analyses confirmed that the material is stable up to 191.0 °C. The dielectric constant, the dielectric loss and AC conductivity were studied as a function of frequency at different temperatures. The higher value of polarizability indicated that the second harmonic generation efficiency was more than that of the standard material KDP.

V. ACKNOWLEDGEMENT

The corresponding author gratefully acknowledges the support from the Department of Science and Technology (DST), Government of India, for the Research project (SB/EMEQ-248/2014).

VI. REFERENCES

- [1]. Oliver SA. *Applied Physics Letters* 76 (2000) 3612.
- [2]. Chinnasamy.E and Senthil. S , *American Institute of Physics*. 1832 (2017) 100019.
- [3]. Dawber.M, Rabe.K.M, *Scott Rev. J, Mod. Phys.*, 77(2005) 1083.
- [4]. Aravindhan. M, Sankaranarayanan. K, Ramamurthy.K, Sanjeeviraja. C, Ramasamy.P, *Thin Solid Films* 477 (2005) 2-6.
- [5]. Venkatesan .A, Arulmani, S, S.Senthil, Rajasaravanan.M.E, *International Journal of Engineering Developemnt and Research*.5 (2017) 480-484.
- [6]. Indumathi. N, Deepa.K, Senthil. S, *International Journal of Engineering Developemnt and Research*.5 (2017) 560-564.
- [7]. Lenin. M, Balamurugan. N, and Ramasamy. P, *Cryst. Res. Technol.* 42 (2007) 39-43.
- [8]. Vivek .P and Murugakoothan .P ,*Appl. Phys.* 115 (2014) 1139-1146.
- [9]. Anie Roshan JosephyCyriac.S, Ittyachem MA. *Materials Letters* 49 (2001) 299-302.
- [10]. Eya. D.D.O, Ekpunobi. A.J, Okeke, *Acad. Open Internet J.* 17 (2006).
- [11]. Maadeswaran.P, Thirumalairajan .S, Chandrasekeran. J, *Optik* 121 (2010) 773.
- [12]. Anandhan. P, Saravanan. T, Vasudevan. S, Mohan Kumar.R, Jeyavel.R, *Cryst. Growth* 312 (2010) 837-841.
- [13]. Goel. N, Sinha. N, Kumar .B, *Opt. Mater.* 35 (2013) 479-486.
- [14]. Surekha.R, Gunaseelan .R, Sagayaraj. P, and Ambujam .K, *Eng. Comm.* 16 (2014) 7979-7989.
- [15]. Sangeetha. V, Gayathri.K, Krishnan.P, Sivakumar .N, Kanangathara. N, and Anbalagan. G, *Crys. Growth.* 389 (2014) 30-38.